Integrated Path Differential Absorption Lidar Optimizations Based on Pre-analyzed Atmospheric Data for ASCENDS Mission Applications

Denis Pliutau, Narasimha S. Prasad (narasimha.s.prasad@nasa.gov)
NASA Langley Research Center, Hampton, VA

Satellite trace gas sensing modeling for missions such as ASCENDS

- Simulation framework to predict performance of trace gas sensing in the atmosphere from space
- Spectroscopic (excitation wavelengths optimizations) and lidar analysis
- Applicable to active sensing missions such as ASCENDS and a variety of molecules including CO_2, CH_4, N_2O etc.
- Projected open source distribution

ASCENDS mission overview

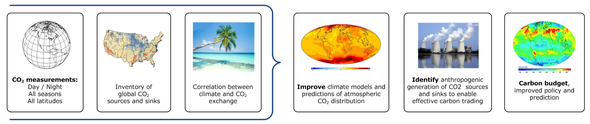

Requirements and approach

- ASCENDS is identified as a medium size Tier II NASA mission in the NRC Decadal Survey and is currently slated for 2019 launch
- ASCENDS will deliver laser based remote sensing measurements of Global CO_2 mixing ratios
- (XCO_2) to a precision of **0.3 percent** on horizontal scales of 100-km over land and 200-km over oceans and passive CO measurements for CO_2 interpretation.
- ASCENDS is the logical extension of OCO and GOSAT

Benefits for climate science

- Quantify global spatial distribution of atmospheric CO_2 on scales of weather models
- Quantify global spatial distribution of terrestrial and oceanic sources and sinks of CO_2 during day/night over all seasons.
- Provide a scientific basis for future projections of CO_2 sources and sinks through data-driven enhancements of Earth-system process modeling.

NASA LaRC ASCENDS approach

- < 0.3% accuracy (~ 1ppm) in CO_2 mixing ratio resolution is required NASA Langley Research Center (LaRC) is developing an **intensity modulated continuous wave (IMCW) laser absorption spectrometer** based remote sensing scheme for the detection of CO_2 at 1.57 microns and O_2 at 1.26 microns from space based platforms
- Multiple wavelengths with differential absorption (DIAL) technique are used 1.26 micron band for O_2 sensing is selected to obtain surface pressure
- 1.26 micron band provides architectural and spectroscopic advantages
- For our experiments two candidate wavelengths in this band will be utilized. Nominally, wavelengths around 1.262 and 1.271 microns have been identified in initial tests lines in these two sub-bands are being further analyzed for sensitivity to environmental parameters

Modeling framework for integrated path space lidar performance estimates

Fig 1.1 Previously under development

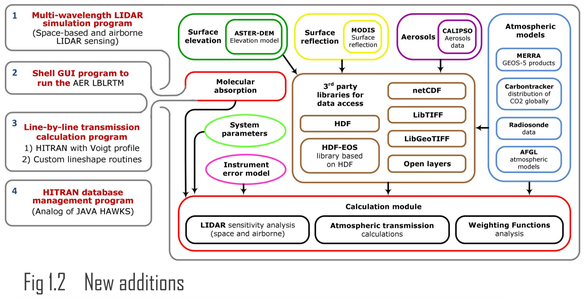

Fig 1.2 New additions

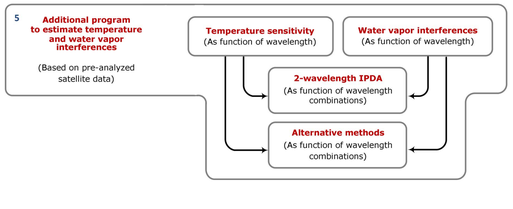

Fig 1.3 Preview GUI screens of the modeling programs

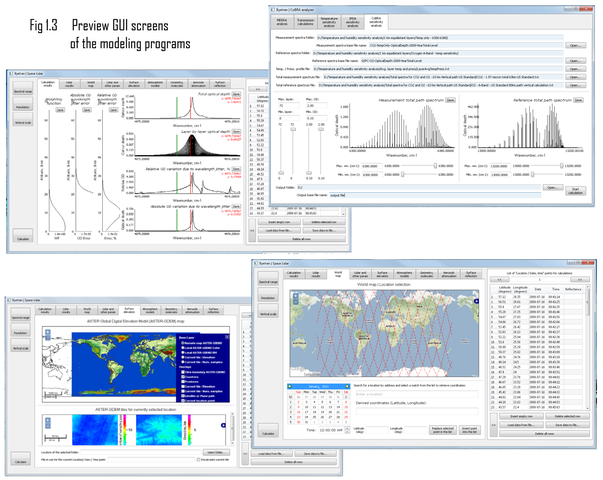

Pre-analyzed atmospheric data for error analysis

Analysis and processing of the MERRA dataset

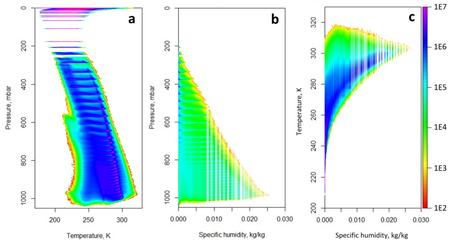

Fig 2.1 Pre-analyzed MERRA atmospheric data

Analysis of pressure, temperature, and humidity fields averaged for all Earth coordinates for a span of year 2009 (the frequency of each combination is color coded on a logarithmic scale of 100 to 10^7).

Grid:
1 Kelvin x 1 mbar x 0.0001 kg/kg
Temperature x Pressure x Humidity

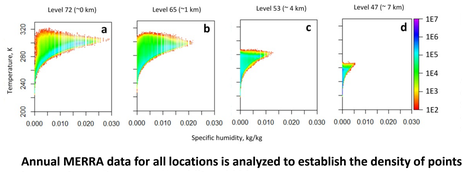

Fig 2.2 Altitude distribution of the analyzed MERRA fields

Analysis of MERRA data at different pressure levels
Showing density of temperature and humidity combinations at selected altitudes

Annual MERRA data for all locations is analyzed to establish the density of points within each temperature x Pressure x Humidity grid bin

Combining individual layer error estimates

Fig 2.3 Averaged temperature and pressure profiles

MERRA atmospheric parameters of pressure and temperature as a function of layer number for the analyzed fields on model layers (inst6_3d_ana_Nv) dataset;.
(a) – Center positions of the total pressure levels as a function of layer number, (b) Annual average of the temperature values for year pressure level as a function of layer number.

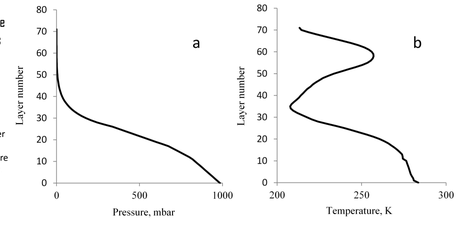

Fig 2.4 Individual layer and combined total path analysis approach

Overview of separate layers analysis methodology based on pre-analyzed MERRA atmospheric fields.

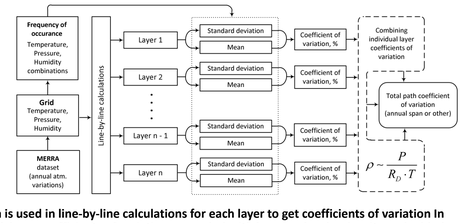

Analyzed MERRA grid data is used in line-by-line calculations for each layer to get coefficients of variation In each layer. Such individual layer coefficients of variation are scaled with layer molecular density and added together to get the total path relative uncertainty.

Global annual temperature sensitivity analysis for CO_2 and O_2 bands

Global annual temperature sensitivity for alternative CO_2 bands

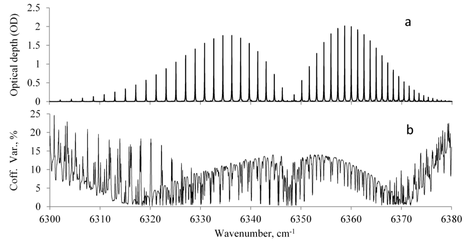

Fig 3.1 Temperature sensitivity analysis for the 1.57 micron CO_2 band

Total absorption spectrum (a) and the temperature induced error (b) for the 1.57 µm band of CO_2 due to annual variations in atmospheric temperature for year 2009.

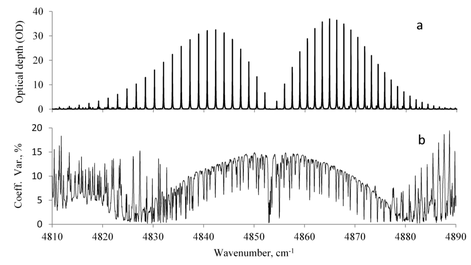

Fig 3.2 Temperature sensitivity analysis for the 2.05 micron CO_2 band

Total absorption spectrum (a) and the temperature induced error (b) for the 2.05 µm band of CO_2 due to annual variations in atmospheric temperature for year 2009.

Preliminary annual cumulative error due to annual global temperature variations

Global annual temperature sensitivity for alternative O_2 bands

Fig 3.3 Temperature sensitivity analysis for the O_2 A-band

Total absorption spectrum (a) and the temperature induced error (b) for the A-Band of O_2 due to annual variations in atmospheric temperature for year 2009.

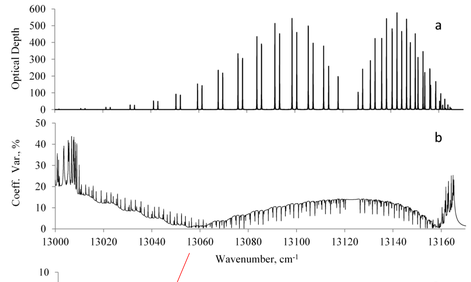

Fig 3.4 Temperature sensitivity analysis for The 1.26-1.27 micron O_2 band

Total absorption spectrum (a) and the temperature induced error (b) for the 1.26-1.27 µm band of O_2 due to annual variations in atmospheric temperature for year 2009.

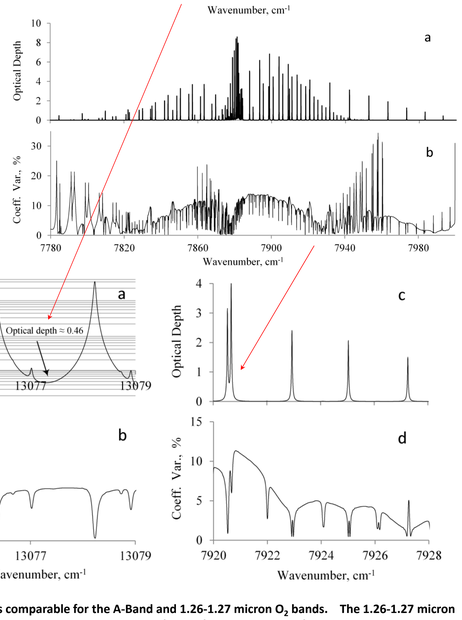

Temperature sensitivity is comparable for the A-Band and 1.26-1.27 micron O_2 bands. The 1.26-1.27 micron band allows achieving lower temperature sensitivities due to closer proximity to line centers.

Wavelength instability effects

Fig 4.1 Laser wavelength jitter analysis example for selected CO_2 spectral lines

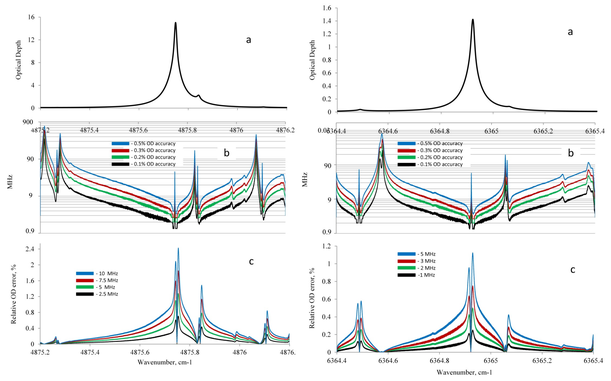

Fig 4.2 Laser wavelength jitter analysis example for selected O_2 spectral lines

Table I Laser wavelength stability requirements in different spectral regions of CO_2 and O_2 molecules to achieve an accuracy of 0.21% in relative optical depth accuracy

Molecule	Center investigating the band	Ref.	Possible lines and wavelengths		Approximate Maximum optical depth	Maximum total jitter for < 0.21% optical depth accuracy		
			Wavenumber, cm^{-1}	Wavelength, nm		MHz	pm	cm^{-1}
O_2	GSFC	1, 2	13075.819	764.7705	0.87	16	0.031	0.00053
O_2	GSFC	1, 2	13075.944	764.7631	1.47	11	0.022	0.00037
O_2	GSFC	1, 2	13076.064	764.7561	3.15	8	0.016	0.00027
O_2	GSFC	1, 2	13077.297	764.684	0.46	1400	2.73	0.047
O_2	LaRC	2	7841.9866 line	1275.1871	1.95 peak	1	0.0054	0.000033
O_2	LaRC	2	7920.596	1262.5312	~ 0.68	130	0.69	0.0043
CO_2	GSFC	2	6359.9674 line	1572.335	~ 1.9 peak	1	0.0082	0.000033
CO_2	LaRC	2	6364.922 line	1571.111	~ 1.38 peak	1	0.0082	0.000033
CO_2	JPL	additional example	4875.6905	2050.992	2.6	2	0.028	0.000067
CO_2	JPL	3	4875.6265	2051.018	0.9	4	0.056	0.00013
CO_2	JPL	4	4875:882	2050.911	0.89	4	0.056	0.00013

Notes: Wavelength positions are approximate based on the data previously reported. The values are presented for specific frequencies or entire lines (marked as "line"). Intensities are specified for either exact wavelength potions or peaks of the lines. The laser jitter is specified for the total wavelength variation span of the laser wavelength.

[1] H. Riris, M. Rodriguez, G. Allan, W. E. Hasselbrack, M. A. Stephen, and J. B. Abshire, "Airborne LIDAR Measurements of Atmospheric Pressure Made Using the Oxygen A-band," in Lasers, Sources, and Related Photonic Devices, OSA Technical Digest (CD) (Optical Society of America, 2012), paper LT2B.5
[2] Susan Kooi, Jianping Mao, James B. Abshire, Edward V. Browell, Clark J. Weaver, Stephen R. Kawa, "Analysis of Vertical Weighting functions for lidar measurements of atmospheric CO_2 and O_2", **A21D**, 2011 AGU Fall Meeting, San Francisco, CA, 2011.
[3] G. Ehret, C. Kiemle, M. Wirth, A. Amediek, A. Fix, S. Houweling, "Space-borne remote sensing of CO_2, CH_4, and N_2O by integrated path differential absorption lidar: sensitivity analysis", Appl. Phys. B, **90**, pp. 593-608, (2008)
[4] Gary D. Spiers, Robert T. Menzies, Joseph Jacob, Lance E. Christensen, Mark W. Phillips, Yonghoon Choi, and Edward V. Browell, "Atmospheric CO_2 measurements with a 2 µm airborne laser absorption spectrometer employing coherent detection," Appl. Opt. **50**, 2098-2111 (2011)

Conclusions and further work

- Framework applicable to any molecule
- Framework operated in the Beta version, further debugging and improvements are ongoing
- Simulation programs are used for the analysis of temperature sensitivity, wavelength stability effects and the weighting functions calculations
- Further analysis and reduction of water vapor interferences is under investigation
- Alternative measurement approaches are being studied
- Verification of the modeling framework components is planned
- The advantages of the implemented methodology is the reduction in required number of calculations (ordinary PC may be used)

References

[1] S. R. Kawa, J. Mao, J. B. Abshire, G. J. Collatz, X. Sun, and C. J. Weaver, "Simulation studies for a space-based CO_2 lidar mission", Tellus B, **62B**, 759-769, (2010)
[2] Robert T. Menzies, and David M. Tratt, "Differential laser absorption spectrometry for global profiling of tropospheric carbon dioxide: selection of optimum sounding frequencies for high-precision measurements", Applied Optics, Vol 42, No. 33, pp. 6569-6577, (2003)
[3] G. Ehret, C. Kiemle, M. Wirth, A. Amediek, A. Fix, S. Houweling,,"Space-borne remote sensing of CO_2, CH_4, and N_2O by integrated path differential absorption lidar: sensitivity analysis", Appl. Phys. B, **90**, pp. 593-608, (2008)